

# Thermonuclear Supernovae: Is Deflagration Triggered by Floating Bubbles?

Eduardo Bravo<sup>1,2</sup> and Domingo García-Senz<sup>1,2</sup>

<sup>1</sup> Dpt. Física i Eng. Nuclear, Universitat Politècnica de Catalunya, Diagonal 647, 08028 Barcelona, Spain

<sup>2</sup> Institut d'Estudis Espacials de Catalunya, Gran Capità 2-4, 08034 Barcelona

**Abstract.** In recent years, it has become clear from multidimensional simulations that the outcome of deflagrations depends strongly on the initial configuration of the flame. We have studied under which conditions this configuration could consist of a number of scattered, isolated, hot bubbles. Afterwards, we have calculated the evolution of deflagrations starting from different numbers of bubbles. We have found that starting from 30 bubbles a mild explosion is produced ( $M(^{56}\text{Ni}) = 0.56\text{M}_\odot$ ), while starting from 10 bubbles the star becomes only marginally unbound ( $K = 0.05$  foes).

## 1 The initial configuration of deflagrations in white dwarfs and its outcomes

The explosion mechanism(s) responsible for thermonuclear supernovae (SNIa) is still not well known. Although there have been recently some claims that the delayed detonation mechanism lacks a physical background, there are still unexplored mechanisms by which the transition from deflagration to detonation could occur (see García-Senz & Bravo, this volume). Here we concentrate on the other possibility, i.e. a pure deflagration that would process about a solar mass, synthesizing of the order of  $0.5\text{M}_\odot$  of  $^{56}\text{Ni}$  in order to make a typical SNIa. Multidimensional calculations of deflagrations bear the advantage over one-dimensional models that the energy generation rate becomes eventually independent from the local value of the flame speed ([5,4], see also Niemeyer, this volume). In these calculations, the acceleration of the fuel consumption rate is due to the deformation of the flame surface, which is well accounted for by 3D hydrocodes.

In this picture, the main free parameter is the initial configuration of the flame. There have been a few [3] simulations of the transition from the hydrostatic phase to the hydrodynamic one, but a self consistent multidimensional initial model is still far from being available. However, a plausible ignition scenario was suggested in [2]: the nearly-simultaneous runaway at several different spots (from here on, bubbles) in the central region of the white dwarf. In this paper, we explore the dependence of the outcome of the explosion on the initial number of bubbles. First, we address the statistics of the initial distribution of bubble radii and, then, we present the results of a couple of hydrodynamical simulations performed with an SPH code ([1] and García-Senz & Bravo, this volume).

### 1.1 Statistical approach to the initial distribution of igniting bubbles

Our statistical approach is based on the following assumptions: **A)** As a result of convection, there appear a number of hot spots, characterized by its central (peak) temperature,  $T_0$ , and its thermal profile (which we take here exponential, with characteristic exponent  $R_0$ ). **B)** Each hot spot evolves adiabatically in place, in a time given by its ignition timescale. **C)** The peak temperatures of the hot spots can be characterized by a statistical continuous function,  $\theta(T_0)$ .

Depending on the thermal gradient inside each hot spot our results can be split into two different regimes: **1)** If the thermal profile is shallow enough, bubbles grow due to spontaneous flame propagation, **2)** otherwise, bubbles grow conductively. In the first case, the distribution function of bubble radii is a time function given by

$$\frac{dN}{dR_b} = \theta(T_0) \frac{A^{1/B} \cdot 10^9}{R_0} \frac{\tau_i(T_{0b}) \exp(BR_b/R_0)}{\{t + \tau_i(T_{0b}) [1 - \exp(BR_b/R_0)]\}^{1+1/B}}, \quad (1)$$

where  $\tau_i(T_{0b}) \sim A (T_{0b}/10^9 \text{ K})^{-B}$  is the ignition timescale, and  $T_{0b} = 10^9 \text{ K}$ . In the second case, the distribution function becomes

$$\frac{dN}{dR_b} = \theta(T_0) \frac{A^{1/B}}{Bv_{cond}} \left( t - \frac{R_b}{v_{cond}} \right)^{1+1/B}. \quad (2)$$

In the first case, and for any reasonable choice of the function  $\theta$ , the resulting distribution has a sharp peak at a determined value of  $R_b$  so that the initial configuration is composed of an arbitrary number of *equal size bubbles*. In contrast, in the second case the bubble radii distribution is continuous up to a maximum radius, which results in a initial distribution of *unequal size bubbles*.

### 1.2 SPH simulations of deflagrations triggered by floating bubbles

Given the constraints that the value of  $R_0$  must satisfy in order to get an initial configuration composed of identical bubbles, we estimate as quite improbable this case. However, for simplicity, here we have adopted this configuration as the starting point of our simulations. We have followed the evolution of the explosion

**Table 1.** Model parameters and results

Model	$N_b$	$R_b$ ( $10^6 \text{ cm}$ )	$M_b$	$E_{kin}$ ( $10^{51} \text{ erg}$ )	$M_{Ni}$ ( $\text{M}_\odot$ )	$M_{C+O}$ ( $\text{M}_\odot$ )	$M_{Si}$ ( $\text{M}_\odot$ )
B30U	30	6.7	2.8%	0.44	0.56	0.65	0.05
B10U	10	9.7	3%	0.05	0.24	0.88	0.04

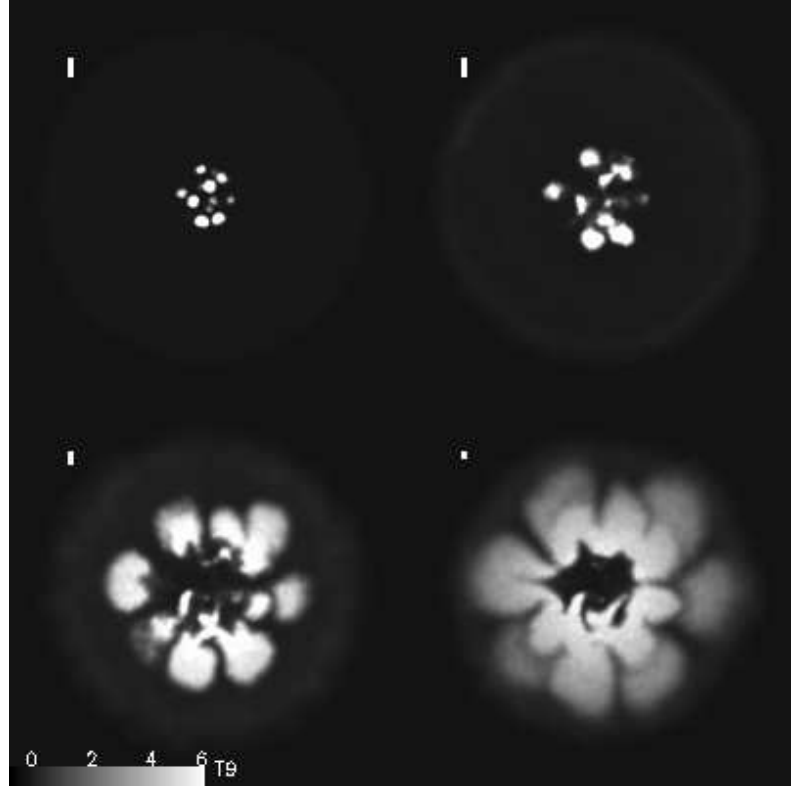


**Fig. 1.** Snapshots of the temperature distribution in a meridian plane at times 0, 0.27, 0.58, and 0.81 s for model B30U. The temperature scale is shown at the bottom left of the image, while the length scale is shown at the top left of each snapshot (the length of the vertical bar is equivalent to 200 km)

of a Chandrasekhar mass white dwarf of initial density  $1.9 \cdot 10^9 \text{ g/cm}^3$  starting from two different numbers of equal size bubbles, as detailed in Table 1 ( $N_b$  is the initial number of bubbles,  $R_b$  its initial radius,  $M_b$  the mass incinerated initially, and the other symbols have their usual meanings). The calculation was performed in 3D with the above mentioned SPH code using 250,000 particles, with a central resolution of 20 km. It is important to emphasize that we did not impose any artificial symmetry conditions and, thus, our model has no artificial characteristic length other than the own resolution of the code. Actually, the imposition of artificial symmetry conditions (for instance, symmetry planes) in any 3D hydrodynamic calculation biases the development of large-scale structures or even of the small-scale ones if they are close enough to a symmetry plane.

The results of our calculations can be found in Table 1 and in Figs. 1 and 2a. The outcome depends strongly on the initial number of bubbles. The deflagration is powered by the evolution and interaction of the bubbles: growth, buoyancy

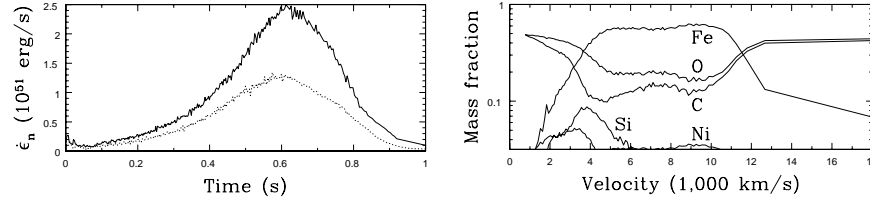


**Fig. 2.** Results of the hydrodynamical calculation. (a) Nuclear energy generation rate as a function of time for models B30U (solid line) and B10U (dotted line). (b) Final distribution of elements in velocity space for model B30U

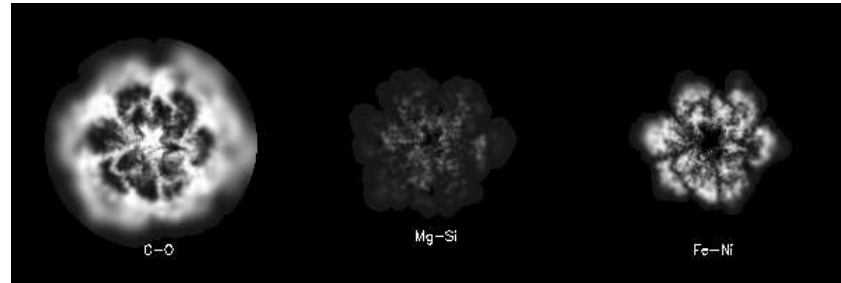


**Fig. 3.** Spatial distribution of the main chemical species at the end of the calculation of model B30U, in the same meridian plane as in Fig. 1

(second snapshot in Fig. 1), and merging (third snapshot). The maximum acceleration of combustion is obtained when the bubbles interact with each other, feeding a rich spectrum of scalelengths to the hydrodynamic instabilities (third snapshot in Fig. 1, see also Fig. 2a). It is not a surprise that this interaction is favoured in the presence of a large number of bubbles. The distribution of nuclei in velocity and space for model B30U is shown in Figs. 2b and 3. Our results agree qualitatively with those obtained in [5].

In summary, our best model (B30U) fails to give the magnitudes adequate for a typical SNIa. A possible cause is a poor representation of the subsonic flame at low densities (a common problem in most SNIa hydrocodes). However, a thorough exploration of the parameter space of initial conditions is in order. This work has been supported by the MCYT grants EPS98-1348 and AYA2000-1785 and by the DGES grant PB98-1183-C03-02.

## References

1. D. García-Senz, E. Bravo, N. Serichol: ApJSS **115**, 119 (1998)
2. D. García-Senz, S.E. Woosley: ApJ **454**, 895 (1995)
3. P. Höflich, J. Stein: ApJ **568**, 779 (2002)
4. A.M. Khokhlov: astro-ph/0008463 (2000)
5. M. Reinecke, W. Hillebrandt, J.C. Niemeyer: astro-ph/0206459 (2002)